

QCD simulations with twisted-mass Wilson quarks

I. Montvay

Deutsches Elektronen-Synchrotron DESY

4th ILFTN Workshop “Lattice QCD via International Research Network”

Sokendai, Shonan Village Center, Japan

March 8 – March 11, 2006

Contents

1. Introduction

lattice actions

ETM Collaboration

2. Phase transition and eigenvalues

positive \leftrightarrow negative quark mass

transition histories

3. Numerical simulations: $N_f = 2$ and $N_f = 2 + 1 + 1$

$$N_f = 2$$

$$N_f = 2 + 1 + 1$$

4. Outlook

Based on:

TWISTED MASS QUARKS AND THE PHASE STRUCTURE OF LATTICE QCD

F. Farchioni, R. Frezzotti, K. Jansen, I. Montvay, G.C. Rossi, E. Scholz, A. Shindler, N. Ukita, C. Urbach, I. Wetzorke,
Eur.Phys.J.C39:421-433,2005, hep-lat/0406039.

THE PHASE STRUCTURE OF LATTICE QCD WITH WILSON QUARKS AND RENORMALIZATION GROUP IMPROVED GLUONS

F. Farchioni, K. Jansen, I. Montvay, E. Scholz, L. Scorzato, A. Shindler, N. Ukita, C. Urbach, I. Wetzorke,
Eur.Phys.J.C42:73-87,2005, hep-lat/0410031.

LATTICE SPACING DEPENDENCE OF THE FIRST ORDER PHASE TRANSITION FOR DYNAMICAL TWISTED MASS FERMIONS

F. Farchioni, K. Jansen, I. Montvay, E.E. Scholz, L. Scorzato, A. Shindler, N. Ukita, C. Urbach, U. Wenger, I. Wetzorke,
Phys.Lett.B624:324-333,2005, hep-lat/0506025.

NUMERICAL SIMULATIONS WITH TWO FLAVORS OF TWISTED-MASS WILSON QUARKS AND DBW2 GAUGE ACTION

F. Farchioni, P. Hofmann, K. Jansen, I. Montvay, G. Muenster, E.E. Scholz, L. Scorzato, A. Shindler, N. Ukita, C. Urbach, U. Wenger,
I. Wetzorke,
hep-lat/0512017.

and work in progress.

Introduction

Numerical simulations of QCD can be performed in the **twisted-mass Wilson fermion** formulation: Aoki, Bitar,... Frezzotti, Grassi, Sint, Weisz,... Frezzotti, Rossi,...

Fermion matrix for an unequal-mass doublet:

with masses $m_u = \mu_\sigma - \mu_\delta$, $m_d = \mu_\sigma + \mu_\delta$

$$\mu_\sigma - \tau_3 \mu_\delta - \frac{1}{2} \sum_{\mu=\pm 1}^{\pm 4} \delta_{y,x+\hat{\mu}} U_{x\mu} \gamma_\mu - i\gamma_5 \tau_1 \left(-\frac{1}{2} \sum_{\mu=\pm 1}^{\pm 4} \delta_{y,x+\hat{\mu}} U_{x\mu} + \mu_{\kappa cr} \right)$$

where the notation $\mu_\kappa \equiv (2\kappa)^{-1} \equiv am_0 + 4$ is used.

More generally: $\mu_{\kappa cr} \rightarrow \mu_\kappa = \mu_{\kappa cr} + (\mu_\kappa - \mu_{\kappa cr})$.

Then the mass term becomes

$$\mu_\sigma - \tau_3 \mu_\delta - i\gamma_5 \tau_1 (\mu_\kappa - \mu_{\kappa cr})$$

This can be diagonalized by a **chiral rotation**:

$$\psi_x \equiv e^{i\frac{\omega}{2}\gamma_5\tau_1}\chi_x = \left(\cos\frac{\omega}{2} + i\gamma_5\tau_1\sin\frac{\omega}{2}\right)\chi_x,$$

$$\bar{\psi}_x \equiv \bar{\chi}_x e^{i\frac{\omega}{2}\gamma_5\tau_1} = \bar{\chi}_x \left(\cos\frac{\omega}{2} + i\gamma_5\tau_1\sin\frac{\omega}{2}\right)$$

After an appropriate chiral transformation the mass term becomes $\mu'_\sigma - \tau_3\mu_\delta$.

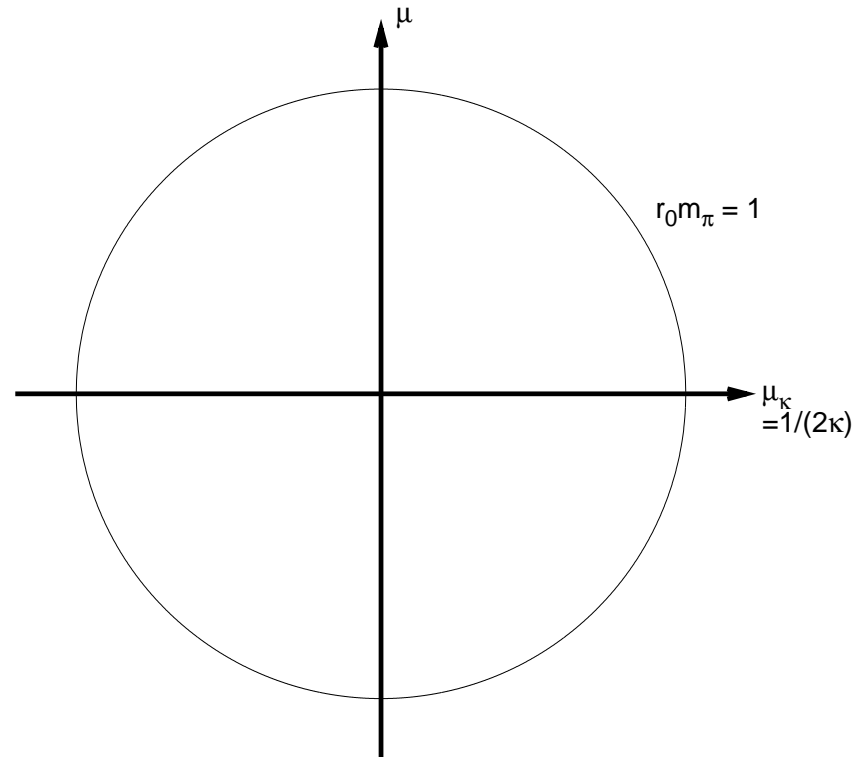
Another conventional notation:

with a chiral transformation and an isospin rotation $\tau_1 \rightarrow \tau_3, \tau_3 \rightarrow -\tau_1$ one obtains

$$S_\chi = \sum_x \left\{ (\bar{\chi}_x [\mu_\kappa + i\gamma_5\tau_3\mu_\sigma + \tau_1\mu_\delta]\chi_x) - \frac{1}{2} \sum_{\mu=\pm 1}^{\pm 4} (\bar{\chi}_{x+\hat{\mu}} U_{x\mu} [r + \gamma_\mu]\chi_x) \right\}$$

$$\equiv \sum_{x,y} \bar{\chi}_y Q_{(\chi)yx}\chi_x$$

In the continuum limit the chiral symmetry is restored and ω becomes irrelevant.



At non-zero lattice spacing the circle is distorted. In the pseudo Goldstone boson sector one can use WChPT: leading lattice artifacts are taken into account.

Sharpe-Singleton,... Sharpe-Shoresh,... Münster, Scorzato, Sharpe-Wu, Aoki-Bär,...

European Twisted Mass Collaboration

Institutes: DESY, INFN Sezione di Roma III, Liverpool University, Milano University, Münster University, Université Paris-Sud, University of Rome “La Sapienza”, Università di Roma Tor Vergata, University of Valencia, ETH Zürich.

IBM p690-Cluster Jump FZ Jülich

Total number of p690 frames: 41,

Total number of processors: 1312,

Aggregate peak performance: 8.9 TFLOPS,

LINPACK performance (41 nodes): 5.568 TFLOPS,

Aggregate main memory: 5.2 TByte,

Cluster interconnect: HPS - High Performance Switch.

IBM Blue Gene/L Jubl FZ Jülich

8 Racks with $(2 \times 16) \times 32$ compute nodes (total 8192),

Compute node: dual processor,

Processortype: 32-bit PowerPC 440 core 700 MHz,

Overall peak performance: 45.8 Teraflops,

Linpack: 36.49 Teraflops,

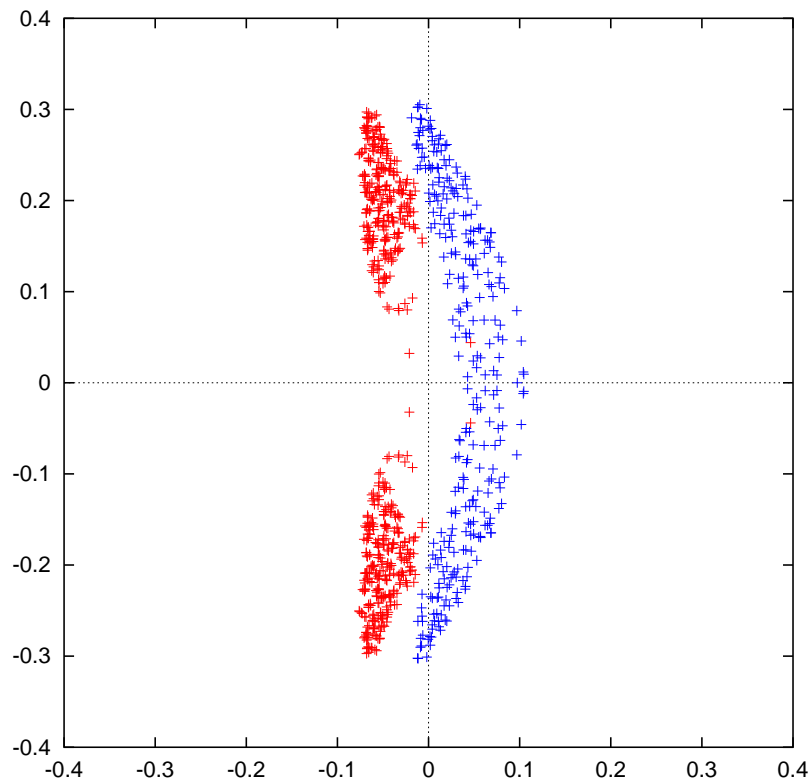
Main memory: 512 Mbytes (aggregate 4.1 TB).

apeNEXT INFN, DESY, Université Paris-Sud:

7+3 apeNEXT racks, with $8 \times 8 \times 8$ processors each.

Phase transition and eigenvalues

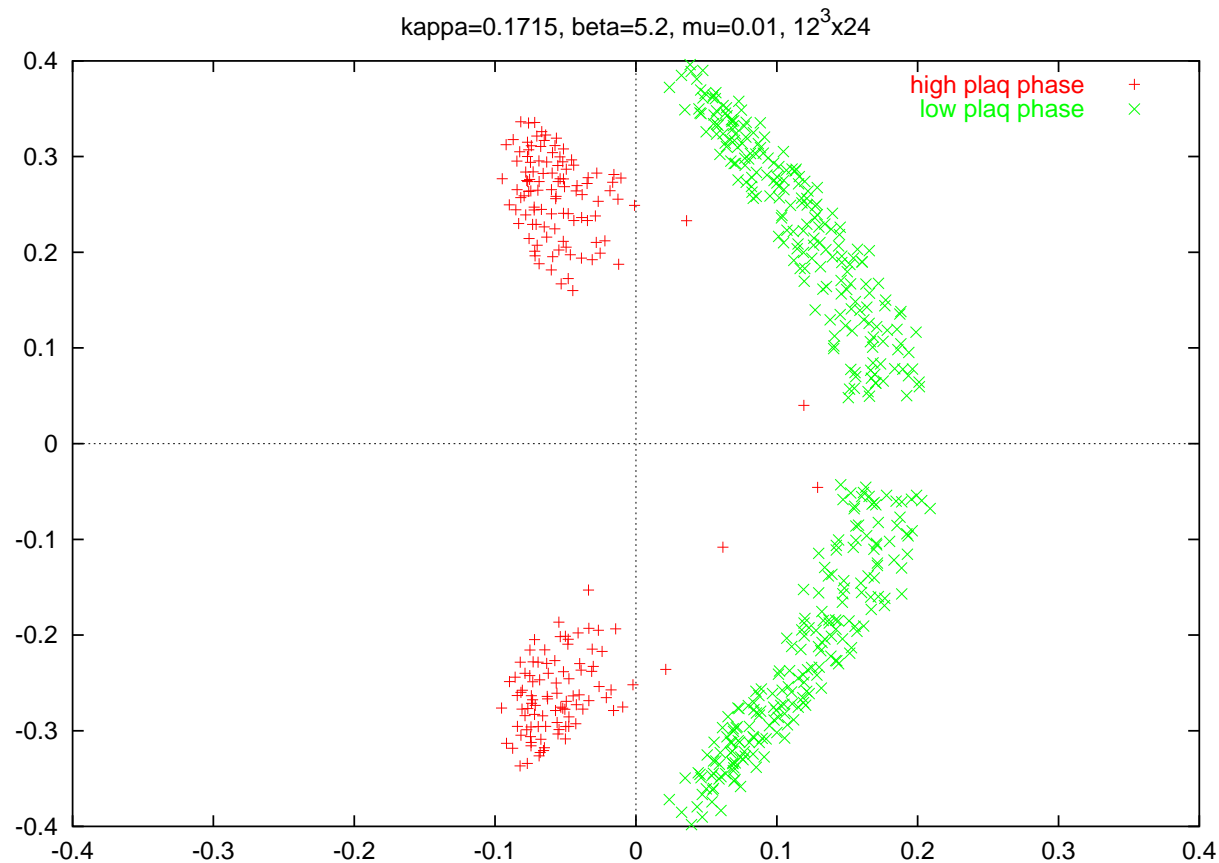
The phase transition at zero quark mass is accompanied by a characteristic change of the eigenvalue spectrum of the Wilson-Dirac fermion matrix.



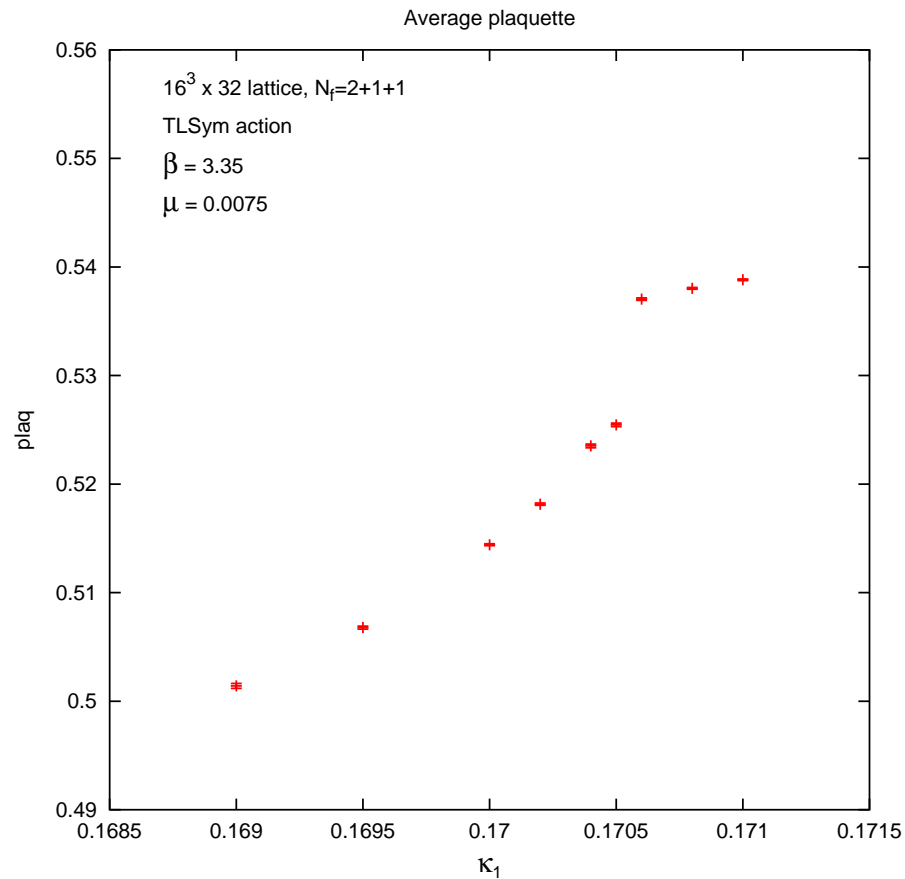
$12^3 \cdot 24$ lattice,
DBW2 gauge action,
 $\beta = 0.67, \kappa = 0.168, \mu = 0$

positive quark mass ($\kappa < \kappa_{cr}$)
negative quark mass ($\kappa > \kappa_{cr}$)

Introducing a non-zero twisted mass: there is a strip without eigenvalues.
negative quark mass ($\kappa > \kappa_{cr}$), positive quark mass ($\kappa < \kappa_{cr}$).

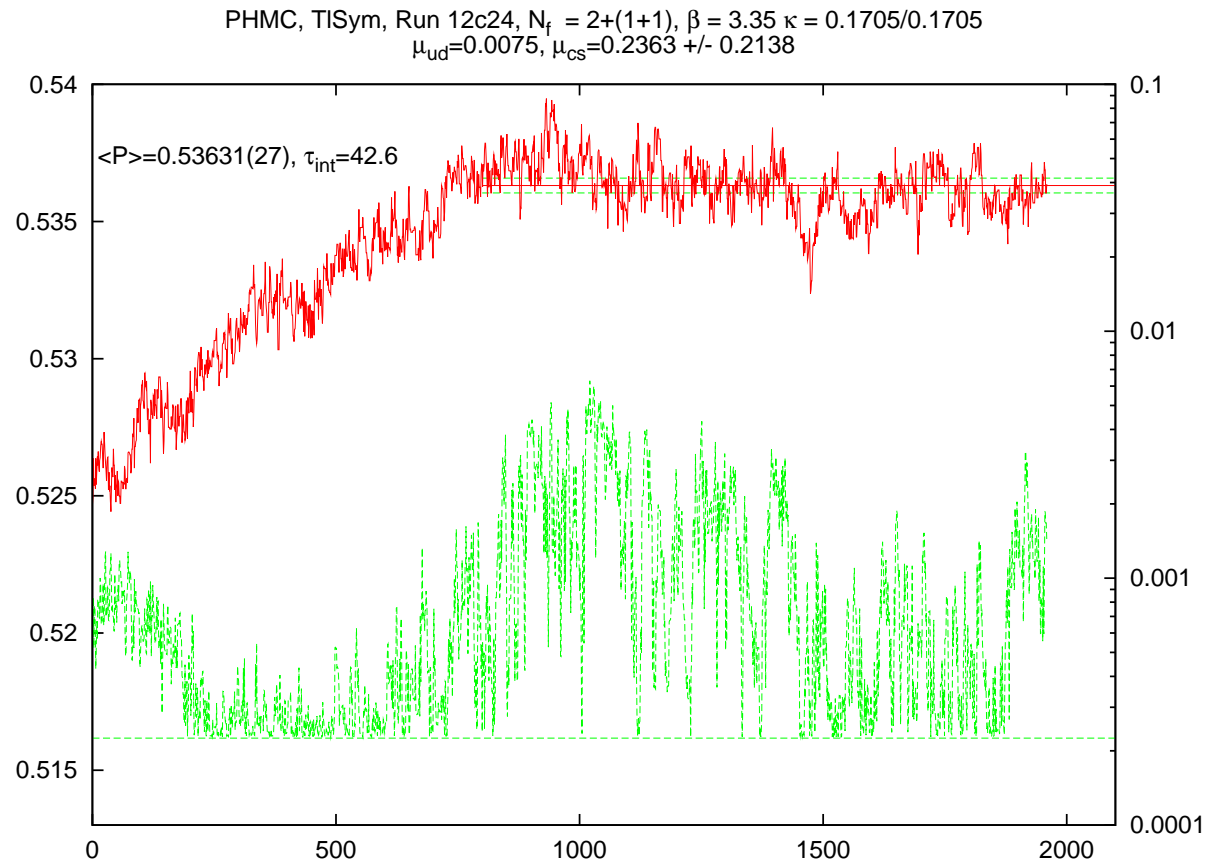


The phase transition at zero quark mass can be seen in the average plaquette because of a chiral-symmetry-breaking mixing with the quark condensate.



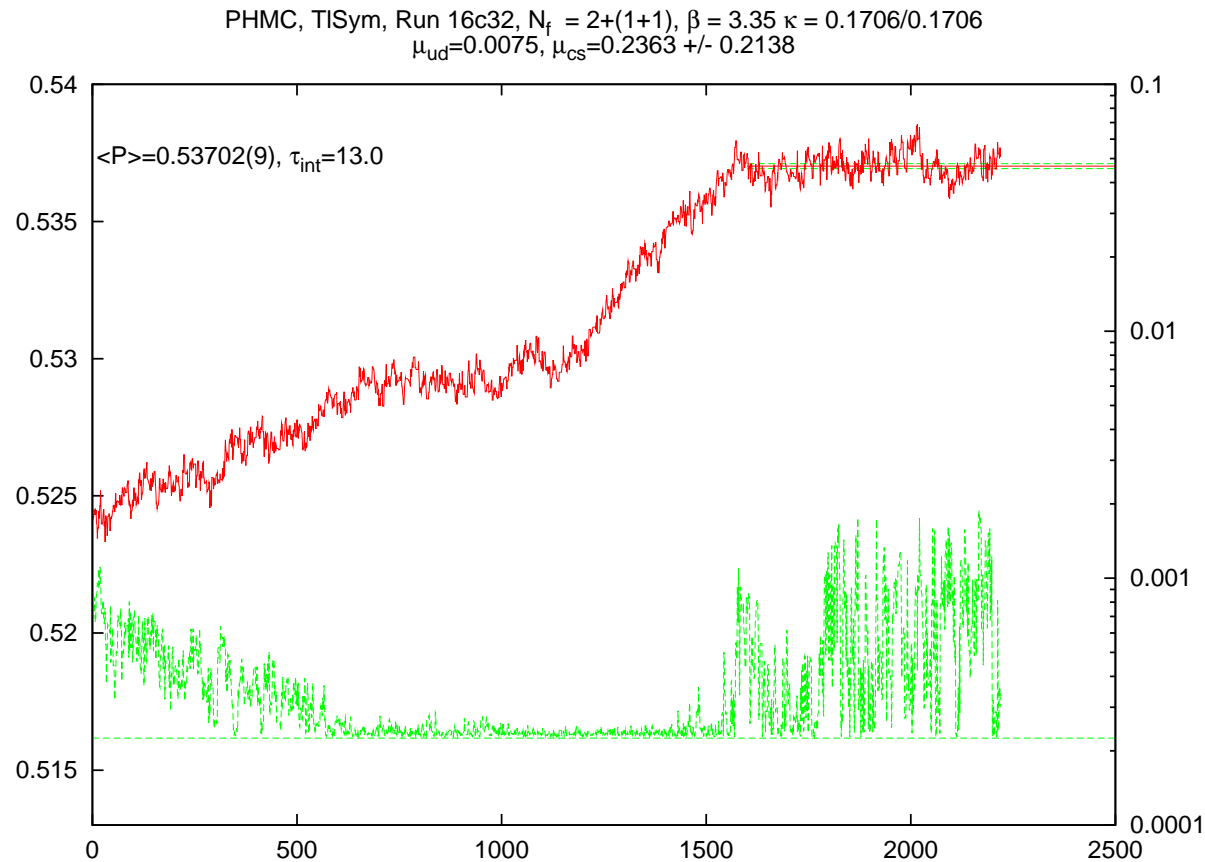
Going across the phase transition: the average plaquette increases due to the chiral-symmetry-breaking mixing with the quark condensate.

red = average plaquette, green = smallest eigenvalue of Q^2 .

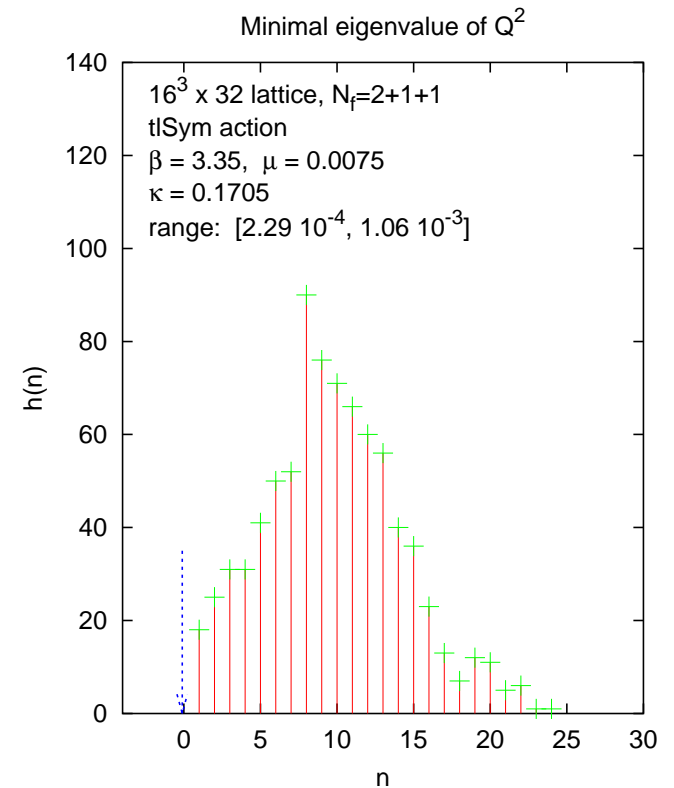
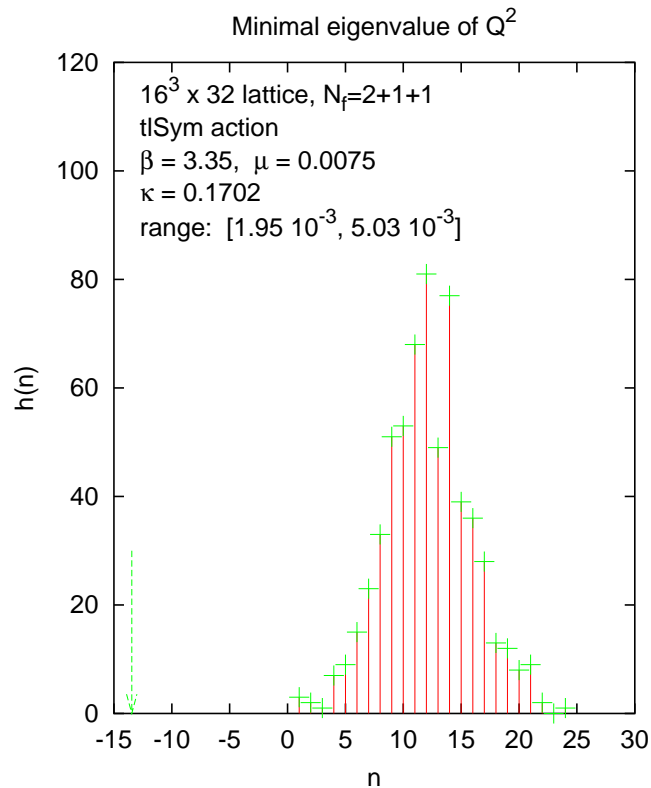


On a larger lattice: it is more difficult to cross. The effect of crossing of the “eigenvalue cloud” can be better seen on the smallest eigenvalue.

red = average plaquette, green = smallest eigenvalue of Q^2 .



The histogram of the smallest eigenvalue of the squared preconditioned fermion matrix. **Left plot: far away from the phase transition, right plot: close to it.**



Numerical simulations: $N_f = 2$ and $N_f = 2 + 1 + 1$

$N_f = 2$ simulations with twisted mass Wilson quarks: (u, d)

Improved gauge actions are used in order to decrease the minimal pion mass which can be simulated at a given lattice spacing:

DBW2 action or tISym = tree level Symanzik-improved action.

First the pion sector is investigated: pion mass, pion decay constant, etc. as a function of the quark mass and volume.

The results can be compared with WChPT which also takes into account leading lattice artifacts.

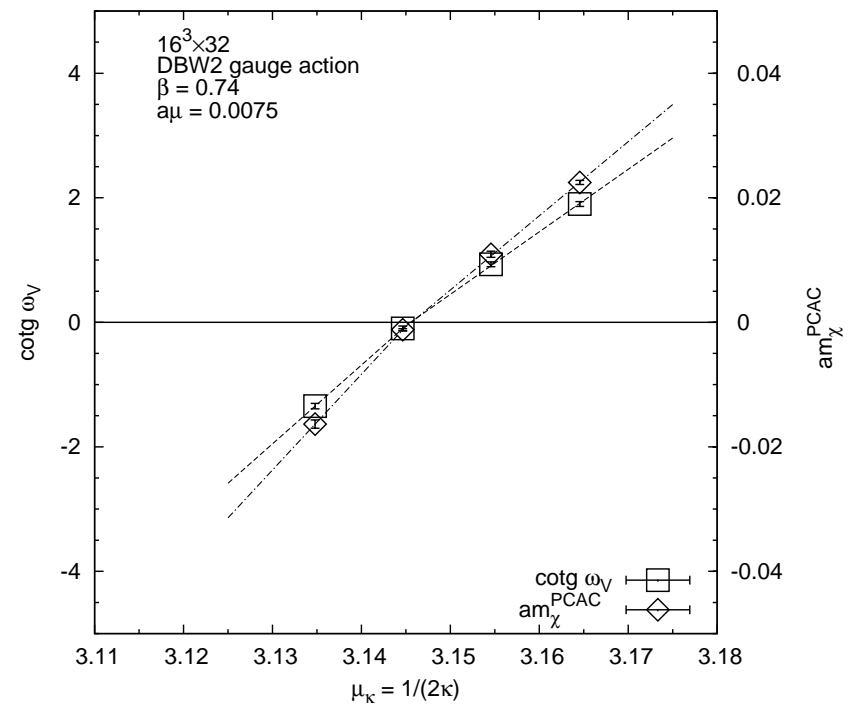
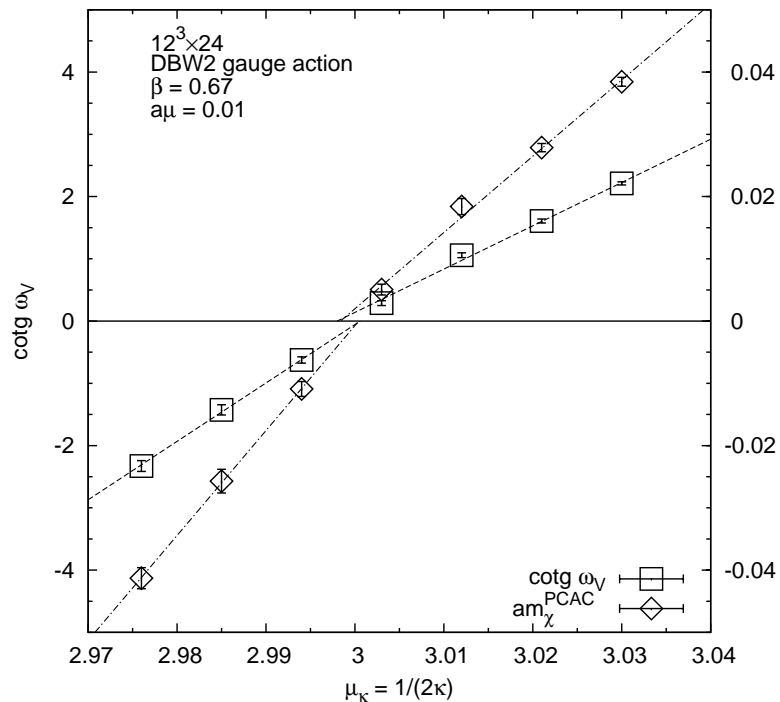
First study on coarse lattices with DBW2 gauge action: hep-lat/0512017.

$12^3 \cdot 24$, $a \simeq 0.17$ fm and $16^3 \cdot 32$, $a \simeq 0.13$ fm at $r_0\mu \simeq 0.028$, $\mu \simeq 11$ MeV.

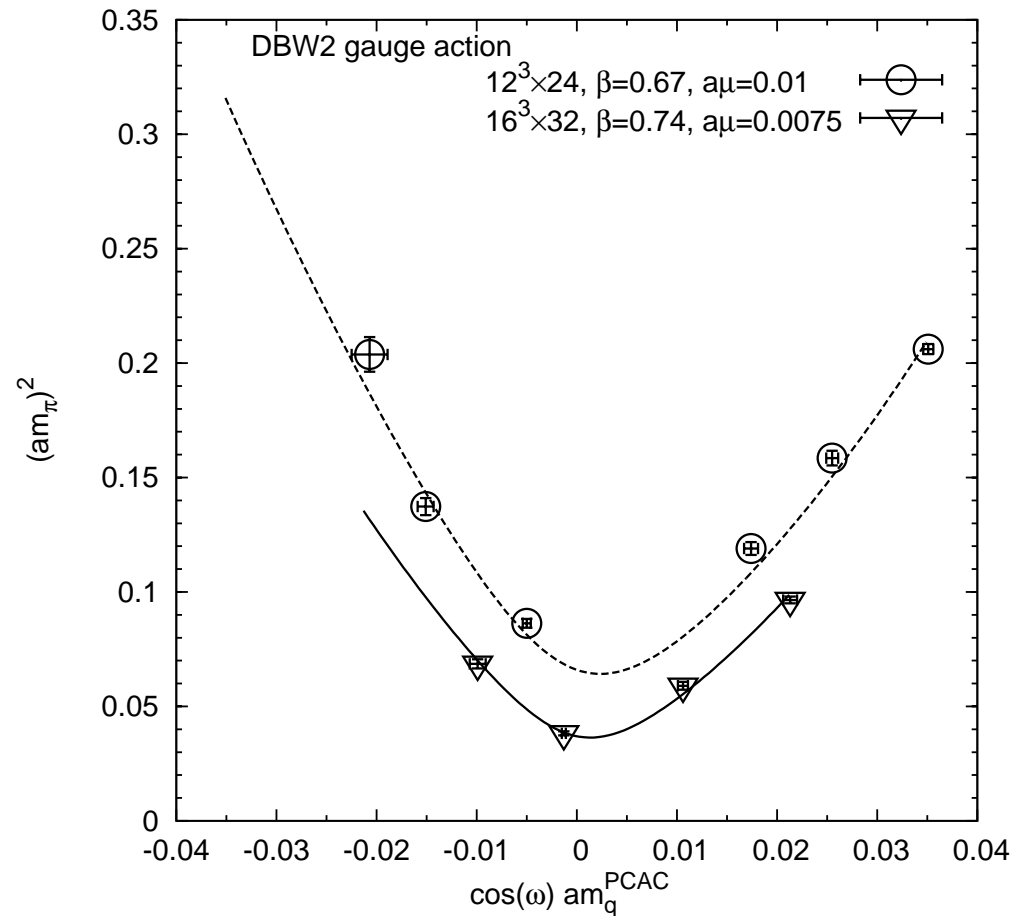
In preparation: tISym gauge action $24^3 \cdot 48$, $a \simeq 0.09$ fm.

Determination of the critical untwisted quark mass (κ_{cr}):
 parity-restoration (squares) and by extrapolating the untwisted PCAC quark
 mass to zero (diamonds). The correct definition of κ_{cr} (“full twist”) is
 important for automatic $\mathcal{O}(a)$ improvement:

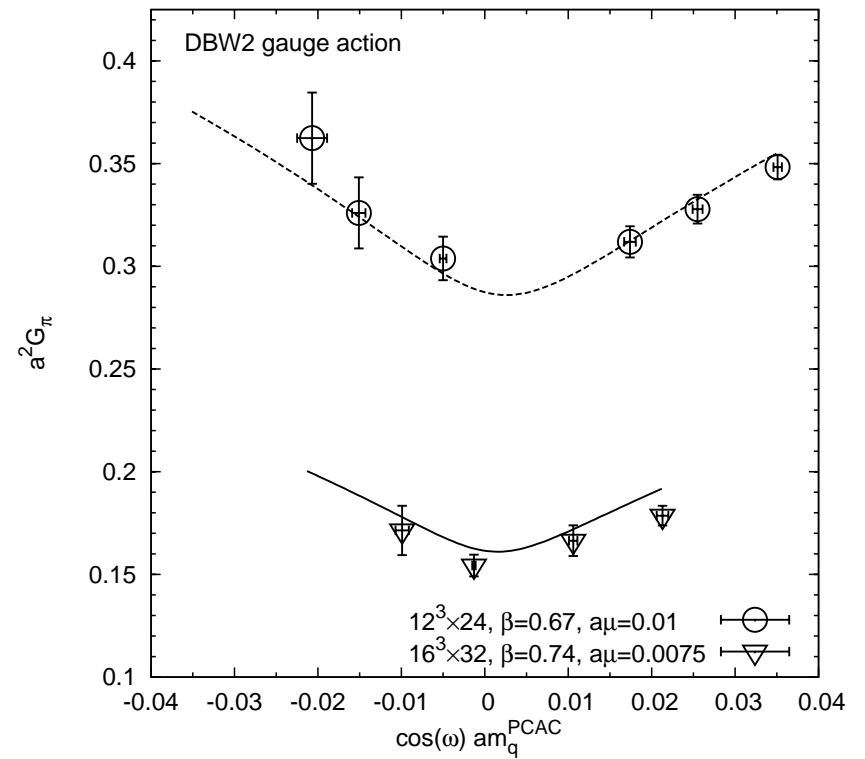
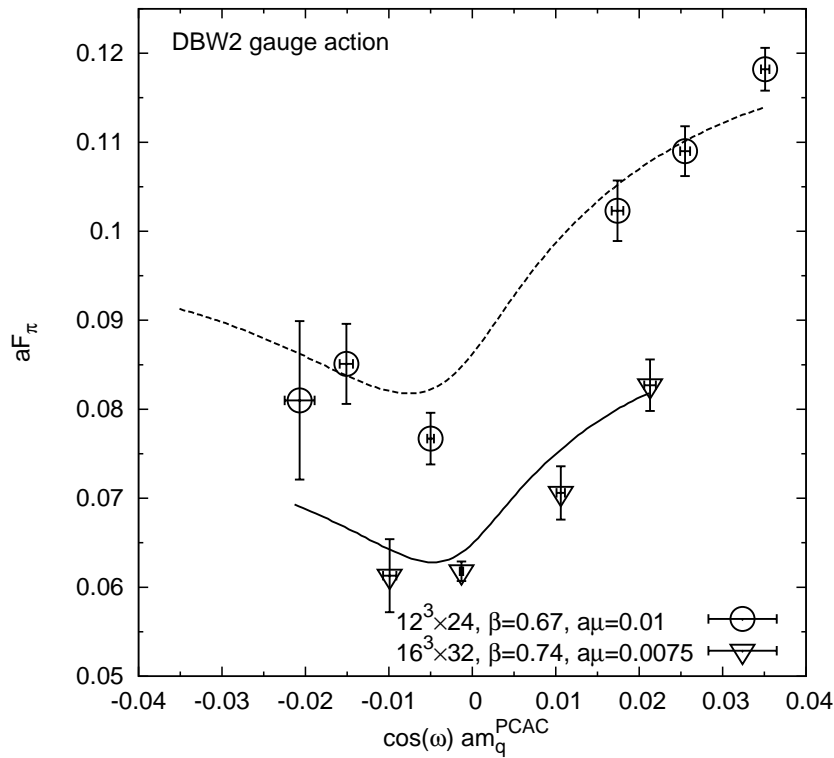
Aoki-Bär, Sharpe-Wu, Frezzotti-Martinelli-Papinutto-Rossi, XLF hep-lat/0411001,...



The simulation results can be qualitatively well fitted by WChPT but because of the coarse lattices and limited statistics of the present data the ChPT parameters cannot be well determined.



The quark mass dependence of the pion decay constant and of the pion matrix element of the pseudoscalar density:



The correct choice of the quark mass parameter is important!

Estimates of the relevant ChPT parameters:

$$2.9 \text{ GeV} \leq B \leq 3.5 \text{ GeV}$$

$$70 \text{ MeV} \leq F_0 \leq 85 \text{ MeV}$$

$$4.0 \leq \Lambda_3/F_0 \leq 8.0$$

$$16.0 \leq \Lambda_4/F_0 \leq 19.0$$

Fits of similar data with the plaquette gauge action are roughly consistent with these values.

The estimates of $\Lambda_{3,4}$ are close to previous estimates of the *qq+q Collaboration*: $\Lambda_3/F_0 \approx 8$, $\Lambda_4/F_0 \approx 21$ and are within the bounds of their phenomenological values given by S. Dürer in hep-lat/0208051:

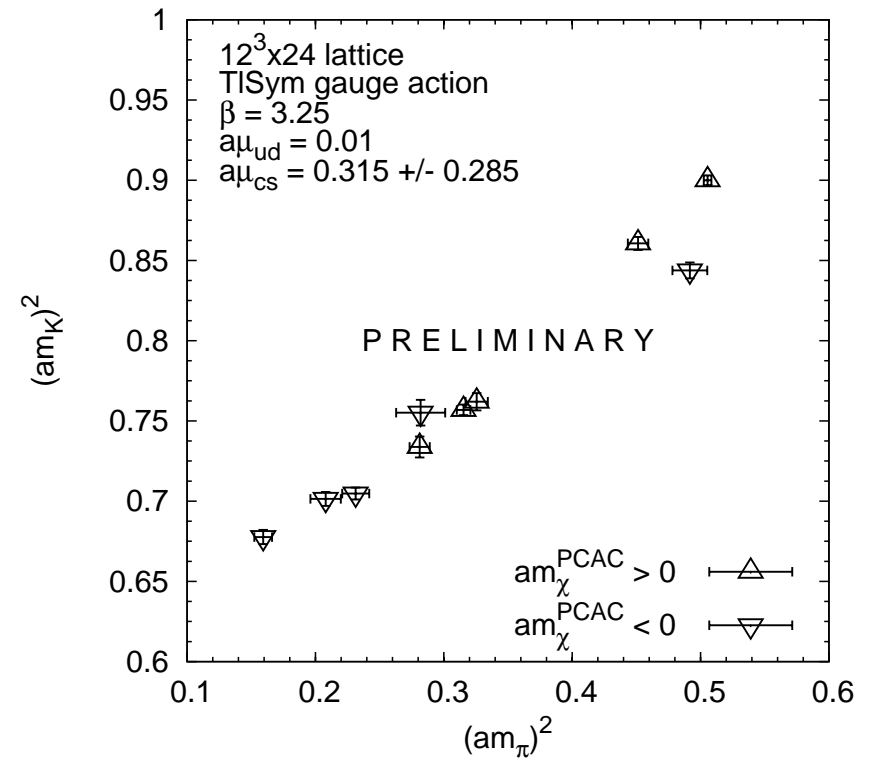
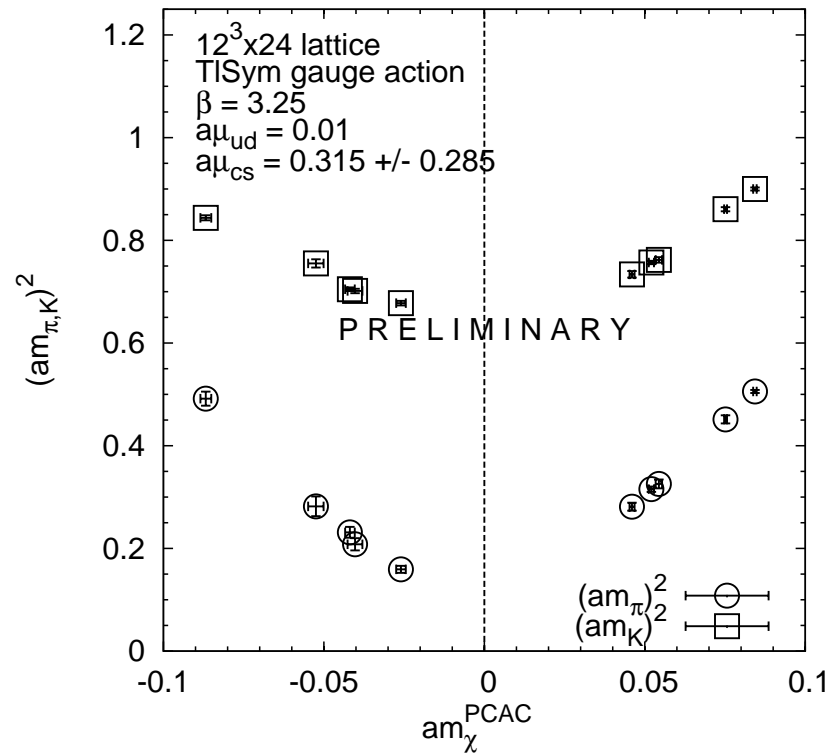
$\Lambda_3 = 0.6 (+1.4, -0.4) \text{ GeV}$, $\Lambda_4 = 1.2 (+0.7, -0.4) \text{ GeV}$ that is

$$2.3 \leq \Lambda_3/F_0 \leq 23.3, \quad 9.3 \leq \Lambda_4/F_0 \leq 22.1.$$

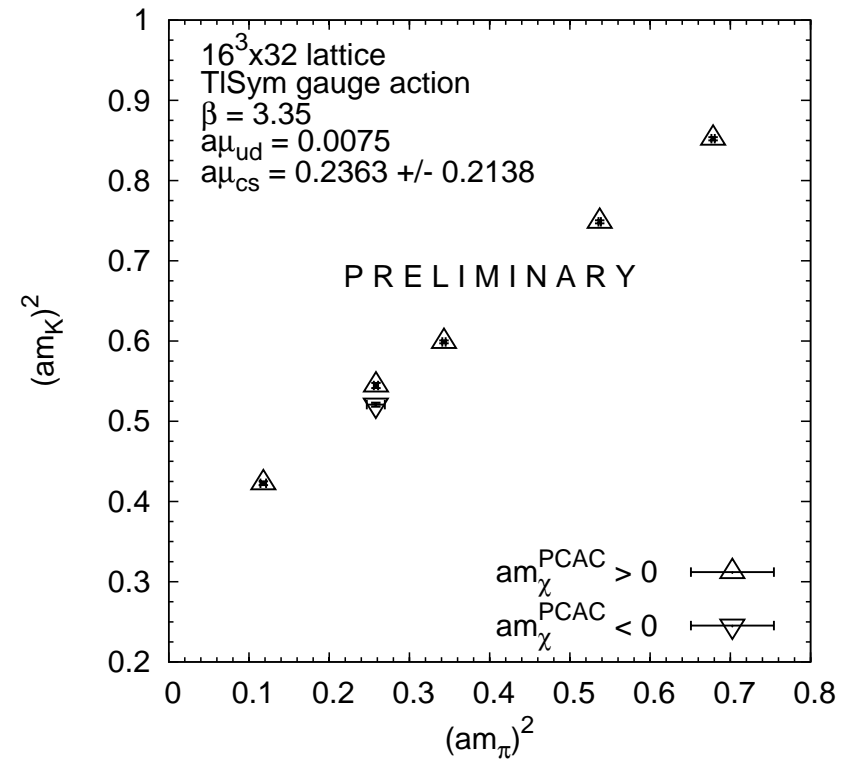
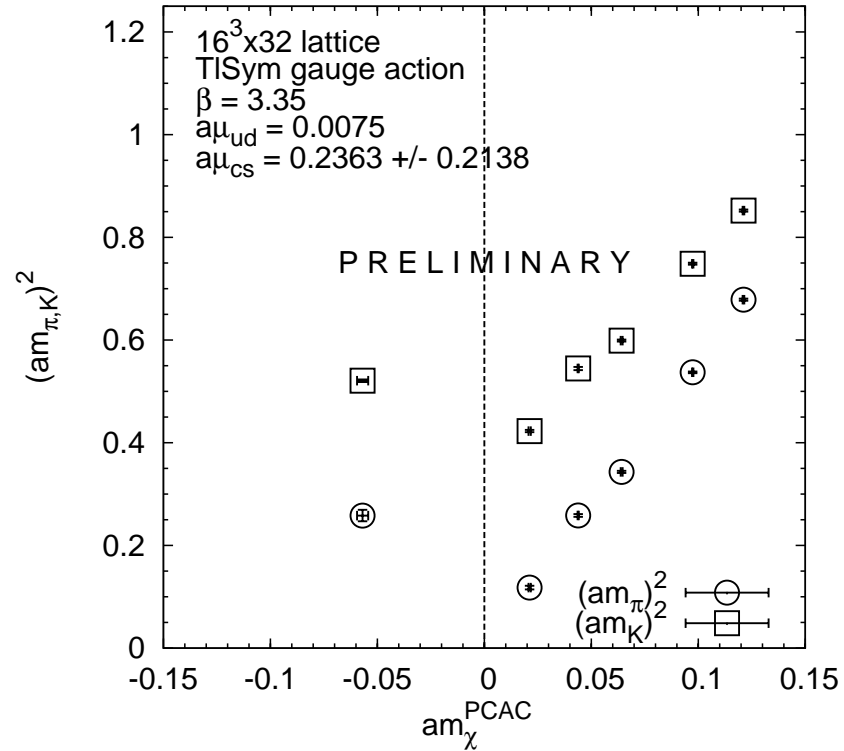
$N_f = 2 + 1 + 1$ simulations with twisted mass Wilson quarks: $(u, d) + c + s$

Unpublished preliminary results by ETMC.

$12^3 \cdot 24$, $a \approx 0.19$ fm:



$16^3 \cdot 32$, $a \approx 0.14$ fm:



The value at $am_{\pi} = 0$ in the second plot roughly gives $m_s \approx 170 - 190$ MeV.

Updating algorithm: PHMC with stochastic correction.

I.M., E. Scholz, hep-lat/0506006

Kaon mass splitting: in a recent paper

STRANGE QUARKS IN QUENCHED TWISTED MASS LATTICE QCD

Abdou M. Abdel-Rehim, Randy Lewis, R.M. Woloshyn, Jackson M.S. Wu, hep-lat/0601036.

a large $K^0 - K^+$ mass splitting is reported in a quenched computation.

In fact, in the Frezzotti-Rossi formulation of mass-split doublets the $K^0 - K^+$ mass splitting is exactly zero.

Taking the twist rotation with the isospin matrix τ_1 and the mass splitting to be diagonal in the direction of τ_3 we have the discrete symmetries:

in the ud quark doublet: $\tau_2 \times Parity$

in the cs quark doublet: $\tau_3 \times Parity$.

Under the combined transformation the K^+ correlator is transformed to the K^0 correlator and similarly in the D -meson doublet.

Therefore there is no isospin breaking in the masses.

Outlook

Advantages of twisted mass LQCD compared to untwisted Wilson-type LQCD:

- the numerical simulation is safer (and faster),
- the lattice artifacts are reduced (“automatic” $\mathcal{O}(a)$ improvement),
- the operator mixing in the renormalization procedure can be made simpler,
- there exists an exactly conserved axialvector current;
- renormalisation Z-factors can be obtained from the twist angle dependence

Disadvantage:

- there is an explicit flavour symmetry breaking (however, the kaon isospin doublet is exactly degenerate).